

# Observation of dipole transitions to a $2^+ \otimes 3^- \otimes$ particle multiplet in $^{143}\text{Nd}$

R.-D. Herzberg, A. Zilges, A.M. Oros,\* and P. von Brentano  
*Institut für Kernphysik, Universität zu Köln,  
 Zùlpicher Strasse 77, D-50937 Köln, Germany*

U. Kneissl, J. Margraf, and H.H. Pitz  
*Institut für Strahlenphysik, Universität Stuttgart, Allmandring 3, D-70569 Stuttgart, Germany*

C. Wesselborg†  
*Institut für Kernphysik, Justus-Liebig-Universität Giessen,  
 Leihgesterner Weg 217, D-35392 Giessen, Germany*  
 (Received 13 September 1994)

A photon scattering experiment on  $^{143}\text{Nd}$  yielded detailed information about the energies, cross sections, and absolute strengths of dipole transitions between 1.4 and 4.1 MeV. Besides some well-known levels at energies around 2 MeV we observed a number of very strong dipole excitations between 2.8 and 3.8 MeV. This is the energy region where one expects the two-phonon- $(2^+ \otimes 3^-) \otimes$  particle multiplet which arises due to the coupling of the unpaired neutron with  $(2^+ \otimes 3^-)$  coupled states in the even-even core nucleus  $^{142}\text{Nd}$ . The summed dipole strength between 2.8 and 3.6 MeV in  $^{143}\text{Nd}$ , according to the sum rule, is comparable to the  $E1$  strength of the  $1^-$  member of the multiplet in the core nucleus  $^{142}\text{Nd}$ . Model calculations in a harmonic approximation with a quadrupole-quadrupole interaction show very good agreement with the experiment and indicate the dominant two-phonon-particle structure  $(2^+ \otimes 3^- \otimes f_{7/2})$  of the excitations in  $^{143}\text{Nd}$ .

PACS number(s): 25.20.Dc, 21.10.Re, 21.60.Ev, 27.60.+j

## I. INTRODUCTION

Octupole excitations of the nucleus have been investigated intensively over recent years [1–5], and it has been proposed that static or dynamic octupole deformations may explain the strong electric dipole transitions observed frequently in nuclei of the rare-earth region and the actinide region [6].

In strongly deformed nuclei the octupole vibration couples to the quadrupole-deformed core. The resulting octupole-vibrational bands are characterized by their  $K$  quantum number [7]. The  $J^\pi=1^-$  bandheads of the  $K=0$  and  $K=1$  bands have been studied extensively in recent photon scattering experiments [8–10]. It has been shown that the  $E1$  ground-state transition strengths of these states are two to three orders of magnitude larger than typical electric dipole transitions in this mass region.

Relatively strong  $E1$  ground-state transitions from  $J=1$  states have also been observed in spherical nuclei. It has been proposed that these dipole excitations arise due to the coupling of the octupole  $3^-$  vibration with the quadrupole  $2^+$  vibration [11–13]. The  $2^+ \otimes 3^-$  structure creates a multiplet of states with  $J^\pi=1^-$  to  $5^-$ .

Whereas the  $1^-$  member of this  $2^+ \otimes 3^-$  multiplet has been observed in different  $N=82$  nuclei [14–16], the experimental information on the other members with  $J>1$  is still rather incomplete. Different experimental techniques have been used to identify the whole two-phonon multiplet [17–20].

Figure 1 shows the summed energy of the lowest-lying  $3^-$  and  $2^+$  states in comparison to the energy of the lowest-lying  $1^-$  states in different Nd isotopes ranging from the spherical vibrational nucleus  $^{142}\text{Nd}$  up to the

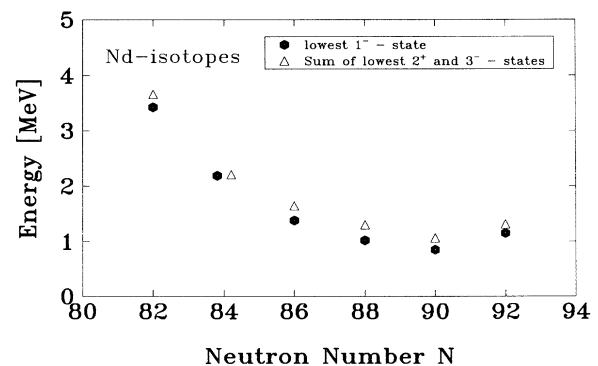


FIG. 1. Comparison of the excitation energies of the lowest  $1^-$  levels (closed hexagons) in the Nd isotopes with the sum energies (open triangles) of the  $2_1^+$  and  $3_1^-$  levels. The correlation between the two quantities is obvious. A similar picture for the Sm isotopes was given by Metzger [15].

\*Permanent address: Institute of Physics and Nuclear Engineering, R-76900 Bucharest-Magurele, Romania.

†Present address: American Physical Society, Editorial Office, 1 Research Road, Ridge, NY 11961.

well deformed rotational nucleus  $^{152}\text{Nd}$ . One can see a strong correlation of the energies independent of the deformation. This correlation points clearly to the octupole structure of the lowest  $1^-$  states.

What are the expected collective excitations in the odd- $A$  neighbor nucleus  $^{143}\text{Nd}$ ? In the ground state the additional neutron is in the  $f_{7/2}$  subshell. If this neutron is coupled to the quadrupole vibration at 1576 keV in the core nucleus  $^{142}\text{Nd}$ , a multiplet of five states with  $J^\pi=3/2^-$  to  $11/2^-$  is expected near the energy of the quadrupole phonon in the core. These levels may mix with single-particle excitations that are close in energy. Similarly the coupling of the single neutron to the  $3^-$  octupole vibration at 2085 keV in  $^{142}\text{Nd}$  should give rise to a multiplet of collective states with  $J^\pi=1/2^+$  to  $13/2^+$  in  $^{143}\text{Nd}$ .

The nucleus  $^{143}\text{Nd}$  has been investigated intensively with different experimental probes. The most complete information stems from a  $^{140}\text{Ce}(\alpha, n\gamma)^{143}\text{Nd}$  study performed by Wrzesinski and co-workers [21] and a proton scattering ( $p, p'$ ) experiment by Trache *et al.* [22]. The latter experiment was especially suited to excite the collective one-phonon-particle states and it was possible to identify all members of the  $3^- \otimes f_{7/2}$  septuplet.

As a next step the unpaired neutron can be coupled to the two-phonon states in the  $N = 82$  nucleus  $^{142}\text{Nd}$ . First evidence for the existence of such an octupole-octupole-particle  $3^- \otimes 3^- \otimes$  particle state has been found in  $^{147}\text{Gd}$  by Kleinheinz *et al.* [23]. In the case of the  $2^+ \otimes 3^-$  excitations the originally five states in  $^{142}\text{Nd}$  will give rise to 31 two-phonon-particle states in  $^{143}\text{Nd}$ . It is evident that one needs an experimental method which is selective in spin and strength to detect these excitations in an energy region where the level density is already very high. Photon scattering<sup>1</sup> fulfills these requirements very well; from the ground state mainly dipole transitions and, to a lesser extent, quadrupole transitions are induced, and the electromagnetic excitation mechanism is sensitive to the radiative decay width  $\Gamma$  of the level. In addition, the method achieves a high energy resolution [full width at half maximum (FWHM)  $\simeq 3$  keV at 3 MeV] and yields absolute transition strengths (i.e., half-lives) when the absolute photon flux is known. Therefore we decided to investigate the nucleus  $^{143}\text{Nd}$  in a photon scattering experiment, the first results of which were recently published in a Letter by our group [24].

The present paper will discuss the results in detail. After a short description of the experimental method in Sec. II we will present the experimental results in Sec. III. Section IV introduces the theoretical model which we used to calculate the two-phonon states and compares the experimental findings with the model calculations. The last section gives a short summary and presents the conclusions.

<sup>1</sup>The terms "photon scattering" and "nuclear resonance fluorescence (NRF)" will be used synonymously throughout the text.

## II. EXPERIMENT AND DATA EVALUATION

The photon scattering experiments have been performed at the bremsstrahlung facility of the Stuttgart Dynamitron [25]. The electron endpoint energy was 4.1 MeV which results in a continuous bremsstrahlung spectrum that decreases exponentially up to the endpoint energy. The photon flux is typically about  $10^6$  photons/(s keV) at energies near 3 MeV. Figure 2 shows the principle of photon scattering. From the ground state with spin  $J_0$  bremsstrahlung induces predominantly dipole transitions to states with  $J = J_0 - 1, J_0$ , and  $J_0 + 1$ ; quadrupole transitions in addition populate levels with  $J = J_0 - 2$  and  $J_0 + 2$ . The deexcitation of the populated states to the ground state and to other excited states is measured with Ge detectors. Throughout this paper we will use the notation  $\Gamma_f$  for the decay widths  $\Gamma(J \rightarrow J_f)$  associated with the decay channel from a state with spin  $J$  to a final state with spin  $J_f$ . The total decay width  $\Gamma$  is the sum of the partial widths over all decay channels,

$$\Gamma = \sum_f \Gamma_f. \quad (1)$$

In our experiment we observe only transitions to the ground state and to the first excited state; thus

$$\Gamma = \Gamma_0 + \Gamma_1. \quad (2)$$

The differential cross section for the resonant scattering of photons of energy  $E$  in a resonance of energy  $E_r$  and width  $\Gamma$  is given by the Breit-Wigner formula

$$\frac{d^2\sigma_{\text{abs}}^0(E)}{d\Omega dE} = \pi\lambda^2 \frac{2J+1}{2(2J_0+1)} \frac{\Gamma_0\Gamma_f}{(E-E_r)^2 + \frac{1}{4}\Gamma^2} \times \frac{W(J, J_0, \Theta)}{4\pi}, \quad (3)$$

where  $\lambda = \hbar c/E_r$ .  $W(J, J_0, \Theta)$  is the angular-correlation function which depends on the spin of the excited state

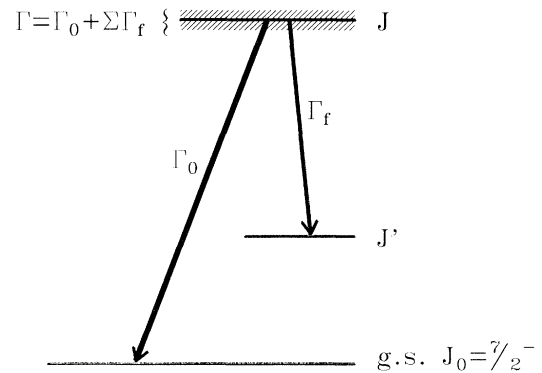


FIG. 2. In photon scattering experiments mainly dipole transitions are induced from the ground state  $J_0$  of the examined isotope. The decay of the populated levels  $J$  back to the ground state ( $\Gamma_0$ ) as well as to other excited levels ( $\Gamma_f$ ) is observed in the experiment. The total width of the excited level is  $\Gamma = \Gamma_0 + \sum \Gamma_f$ .

and of the final state as well as on the angle  $\Theta$  extended by the bremsstrahlung beam, the target, and the Ge detector.  $\Gamma_0$  and  $\Gamma_f$  denote the partial decay widths to the ground state and other states, respectively. Integrating over the energy one gets the total differential cross section for bremsstrahlung scattering,

$$I_s = \frac{d\sigma}{d\Omega} = \pi^2 \lambda^2 \frac{2J+1}{2J_0+1} \Gamma_0 \frac{\Gamma_f}{\Gamma} \frac{W(J, J_0, \Theta)}{4\pi}. \quad (4)$$

Photon scattering spectra of the isotopically enriched  $^{143}\text{Nd}$  target were recorded simultaneously under angles of approximately  $90^\circ$ ,  $130^\circ$ , and  $150^\circ$ . Figure 3 shows the angular-correlation functions for the various possible spin cascades assuming pure dipole radiation. As the angular-correlation functions are nearly identical it was not possible to determine the spin of the excited states with the present statistics of the measurements. Therefore, we evaluate the spectrum recorded at  $130^\circ$  where  $W(J, J_0, \Theta) \simeq 1.0$  for all possible spin cascades in order to calculate the integrated cross section  $I_s$ . From  $I_s$  we extract the spin-dependent ground-state decay width

$$\frac{1}{8}(2J+1)\Gamma_0 = \frac{1}{(\pi\hbar c)^2} \left(1 + \frac{\Gamma_1}{\Gamma_0}\right) E_r^2 I_s. \quad (5)$$

Here  $\Gamma_1/\Gamma_0$  is the measured branching ratio to the first excited state. The factor  $\frac{1}{8} = (2J_0+1)^{-1}$  arises from the ground-state spin  $J_0 = 7/2$  in  $^{143}\text{Nd}$ . For dipole excitations in  $^{143}\text{Nd}$  the spin factor takes on the values  $(2J+1) = 6, 8,$  and  $10$  for the spins  $J = 5/2, 7/2,$  and  $9/2$ , respectively.

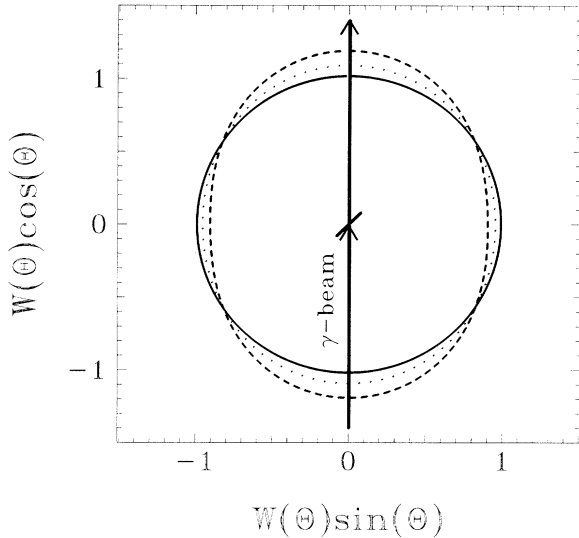


FIG. 3. Angular-correlation functions for the different possible spin cascades in  $^{143}\text{Nd}$  assuming pure dipole or quadrupole character. The overlapping solid lines indicate cascades of the type  $7/2 \rightarrow 3/2 \rightarrow 7/2$  or  $7/2 \rightarrow 5/2 \rightarrow 7/2$ , the dashed line indicates a  $7/2 \rightarrow 7/2 \rightarrow 7/2$  cascade, and the dotted line corresponds to cascades of the type  $7/2 \rightarrow 9/2 \rightarrow 7/2$  or  $7/2 \rightarrow 11/2 \rightarrow 7/2$ . All functions are identical for an observation angle of  $127^\circ$  with respect to the incoming photon beam.

To obtain the absolute transition strengths  $B(E1)$ ,  $B(M1)$ , or  $B(E2)$  (neglecting possible admixtures of other multiplicities),  $\Gamma_0$  is normalized with the transition energy

$$B(\Pi\lambda)\downarrow = B(\Pi\lambda; J \rightarrow J_0) = b_{\pi\lambda} \frac{\Gamma_0}{E_r^{2\lambda+1}} := b_{\pi\lambda} \Gamma_0^{\text{red}}, \quad (6)$$

where  $b_{\pi\lambda}$  is a constant depending on the parity and multipolarity of the transition. While the ground-state transition width  $\Gamma_0$  can only be extracted from our experiment as  $\frac{2J+1}{2J_0+1}\Gamma_0$ , the  $B(\Pi\lambda)\uparrow$  values are again independent of the spin:

$$\begin{aligned} B(\Pi\lambda; J_0 \rightarrow J) &= \frac{2J+1}{2J_0+1} B(\Pi\lambda; J \rightarrow J_0) \\ &= \frac{2J+1}{2J_0+1} \frac{\Gamma_0}{E_r^{2\lambda+1}} b_{\pi\lambda} \\ &= \frac{1}{(\pi\hbar c)^2} \frac{I_s}{E_r^{2\lambda-1}} \left(1 + \frac{\Gamma_1}{\Gamma_0}\right) b_{\pi\lambda}. \end{aligned} \quad (7)$$

For the three types of transitions we have considered (i.e.,  $E1$ ,  $M1$ , and  $E2$ ) we obtain from Eq. (6) the relations

$$B(E1)\uparrow [e^2 \text{fm}^2] = 0.955 \times 10^{-3} \Gamma_0^{\text{red}} [\text{meV}/\text{MeV}^3], \quad (8)$$

$$B(M1)\uparrow [\mu_N^2] = 0.0864 \Gamma_0^{\text{red}} [\text{meV}/\text{MeV}^3], \quad (9)$$

$$B(E2)\uparrow [e^2 \text{fm}^4] = 1245 \Gamma_0^{\text{red}} [\text{meV}/\text{MeV}^5]. \quad (10)$$

### III. EXPERIMENTAL RESULTS

Tables I and II summarize the experimental results from our photon scattering experiment on  $^{143}\text{Nd}$ . The error in the excitation energy  $E_x$  is  $\leq 1$  keV. The angular-correlation coefficient  $W_{95}/W_{130}$  is determined from the normalized peak areas detected under  $95^\circ$  and  $130^\circ$ . If one assumes either pure dipole or pure quadrupole character for the depopulating transition, one expects in both cases a value  $W_{95}/W_{130} \simeq 0.95$  which is in agreement with most of the measured ratios.

The integrated cross sections  $I_s$  of the states are determined directly from the measured peak areas through a normalization to the detector efficiency and to the absolute photon flux. The absolute photon flux is determined from the simultaneously measured  $^{27}\text{Al}$  calibration target. A recent self-absorption measurement on  $^{27}\text{Al}$  confirmed the lifetimes of the levels, from which the level widths and thus the cross sections can be deduced. These lifetimes were used for the calibration of the present experiment [26]. Due to a lack of Al calibration lines below 2.2 MeV, the integrated cross sections of levels in  $^{143}\text{Nd}$  with low excitation energies have a large systematic error.

The next columns of Tables I and II give the ground-state decay widths  $\Gamma_0$ . In Table I the spins of the excited states are known and we can give the reduced ground-state decay widths  $\Gamma_0/E_x^3$  from which the corresponding  $B(\Pi\lambda)$  values are easily computed using Eqs. (8)–(10). In Table II we give the  $B(\Pi\lambda)$  values under the assumption of electric dipole character. Reduced ground-state

TABLE I. Energies, spins, and parities  $J^\pi$ , strength ratios under  $95^\circ$  and  $130^\circ$ , integrated cross sections  $I_s$ , ground-state decay widths  $\Gamma_0$ , and energy-reduced ground-state decay widths  $\Gamma_0^{\text{red}}$  for levels observed in  $^{143}\text{Nd}$  with spins known from other experiments. The appropriate  $B(\Pi\lambda; J_0 \rightarrow J)$  values are easily deduced from the table using Eqs. (8)–(10).

Energy (MeV)	$J^\pi$	$\Pi\lambda$	$W_{95}/W_{130}$	$I_s$ (eV b)	$\Gamma_0$ (meV)	$\Gamma_0^{\text{red}}$ (meV/MeV $^{2\lambda+1}$ )	Remarks
1.407	$9/2^-$	$E2$	$0.84 \pm 0.24$	$20.7 \pm 6.7$	$8.6 \pm 2.8$	$1.56 \pm 0.50$	<sup>a</sup>
1.431	$11/2^-$	$E2$	$0.65 \pm 0.25$	$18.9 \pm 6.3$	$6.7 \pm 2.2$	$1.12 \pm 0.37$	<sup>a</sup>
1.555	$5/2^-$	$E2$	$1.11 \pm 0.17$	$25.9 \pm 7.3$	$21.8 \pm 6.1$	$2.39 \pm 0.67$	<sup>b,c</sup>
1.739	$9/2^-$	$E2$	$0.57 \pm 0.25$	$11.3 \pm 3.2$	$7.1 \pm 2.0$	$0.44 \pm 0.12$	<sup>b,c</sup>
1.851	$7/2^-$	$E2$	$1.38 \pm 0.33$	$10.2 \pm 2.9$	$9.2 \pm 2.6$	$0.42 \pm 0.12$	<sup>b</sup>
1.911	$5/2^-$	$E2$	$1.58 \pm 0.61$	$5.4 \pm 1.5$	$6.8 \pm 1.8$	$0.27 \pm 0.07$	<sup>a</sup>
1.995	$5/2^+$	$E1$	$1.90 \pm 0.96$	$4.1 \pm 1.7$	$5.7 \pm 2.3$	$0.72 \pm 0.29$	<sup>a</sup>
2.011	$9/2^+$	$E1$	$1.03 \pm 0.14$	$20.4 \pm 1.8$	$17.2 \pm 1.5$	$2.12 \pm 0.19$	<sup>a</sup>
2.091	$7/2^+$	$E1$	$2.63 \pm 1.70$	$2.3 \pm 1.2$	$15 \pm 8$	$1.6 \pm 0.9$	<sup>b,c</sup>
2.222	$5/2^+$	$E1$	$2.35 \pm 0.81$	$3.6 \pm 0.9$	$6.2 \pm 1.6$	$0.57 \pm 0.15$	<sup>a</sup>
2.317	$(7/2)^\pi$	$(E1, M1)$	$1.86 \pm 1.55$	$2.0 \pm 1.0$	$2.7 \pm 1.4$	$0.22 \pm 0.11$	<sup>a</sup>
2.558	$(9/2)^+$	$E1$	$0.88 \pm 0.20$	$13.7 \pm 2.5$	$18.6 \pm 3.4$	$1.11 \pm 0.20$	<sup>a</sup>

<sup>a</sup> $J^\pi$  from Ref. [32].

<sup>b</sup> $J^\pi$  from Ref. [21].

<sup>c</sup>Branching ratio was taken from Ref. [21].

decay widths as well as  $B(\Pi\lambda)$  values depend on possible branchings to states other than the ground state. If no branching is observed in our experiment but information from other studies exists, we discuss the influence in the text. In Table II the states with unknown spins are summarized. Following the arguments in the previous section, we give the spin dependent decay widths  $g\Gamma_0$

TABLE II. Energies, strength ratios under  $95^\circ$  and  $130^\circ$ , integrated cross sections  $I_s$ , ground-state decay widths  $g\Gamma_0$ , and  $B(\Pi\lambda; J_0 \rightarrow J)$  values for hitherto unknown levels in  $^{143}\text{Nd}$ . We use  $g\Gamma_0 = \frac{2J+1}{2J_0+1}\Gamma_0$ . Although the multiplicities are not known, we compute  $B(\Pi\lambda; J_0 \rightarrow J)$  values under the assumption of  $\Pi\lambda = E1$ .

Energy (MeV)	$W_{95}/W_{130}$	$I_s$ (eV b)	$g\Gamma_0$ (meV)	$B(\Pi\lambda; J_0 \rightarrow J)$ ( $10^{-3} e^2 \text{ fm}^2$ )
1.690	$1.02 \pm 0.25$	$14.7 \pm 4.8$	$10.9 \pm 3.6$	$2.16 \pm 0.72$
2.415	$1.17 \pm 0.47$	$4.9 \pm 1.1$	$7.4 \pm 1.7$	$0.51 \pm 0.11$
2.493	$1.29 \pm 0.43$	$4.4 \pm 1.0$	$7.1 \pm 1.6$	$0.44 \pm 0.10$
2.554	$1.34 \pm 0.54$	$3.5 \pm 1.2$	$6.0 \pm 2.0$	$0.34 \pm 0.11$
2.629	$1.02 \pm 0.64$	$2.3 \pm 0.8$	$4.2 \pm 1.4$	$0.22 \pm 0.08$
2.926	$1.03 \pm 0.07$	$35.6 \pm 2.5$	$79.3 \pm 5.7$	$3.03 \pm 0.22$
2.968	$0.55 \pm 0.13$	$11.9 \pm 1.4$	$27.4 \pm 3.1$	$1.00 \pm 0.11$
3.046	$0.78 \pm 0.12$	$14.1 \pm 1.3$	$34.0 \pm 3.2$	$1.15 \pm 0.11$
3.073	$1.07 \pm 0.20$	$9.9 \pm 1.3$	$24.4 \pm 3.1$	$0.80 \pm 0.11$
3.081	$0.96 \pm 0.32$	$4.8 \pm 1.0$	$12.0 \pm 2.5$	$0.39 \pm 0.09$
3.089	$1.74 \pm 0.49$	$4.1 \pm 1.0$	$10.3 \pm 1.2$	$0.33 \pm 0.04$
3.214 <sup>a</sup>	$0.80 \pm 0.28$	$4.2 \pm 1.0$	$44.7 \pm 10.2$	$1.29 \pm 0.30$
3.246	$0.93 \pm 0.10$	$24.1 \pm 2.2$	$66.1 \pm 6.0$	$1.84 \pm 0.17$
3.269	$0.85 \pm 0.14$	$16.7 \pm 1.6$	$46.5 \pm 4.5$	$1.27 \pm 0.12$
3.317	$0.83 \pm 0.33$	$9.2 \pm 1.2$	$26.4 \pm 3.6$	$0.69 \pm 0.10$
3.448	$1.00 \pm 0.33$	$6.4 \pm 1.4$	$19.7 \pm 4.4$	$0.46 \pm 0.11$
3.519	$0.52 \pm 0.24$	$8.1 \pm 1.3$	$26.1 \pm 4.3$	$0.57 \pm 0.10$
3.759	$1.41 \pm 0.35$	$11.6 \pm 2.1$	$42.5 \pm 7.8$	$0.76 \pm 0.14$

<sup>a</sup>Branching to  $3/2^-$  level at 742 keV observed.

where the spin dependent factor is  $g = \frac{1}{8}(2J + 1)$ .

A typical NRF spectrum of  $^{143}\text{Nd}$  is shown in Fig. 4. The strong line at 2.982 MeV originates from the calibration standard  $^{27}\text{Al}$ .

### A. States with known spins

We will start by discussing the results summarized in Table I which gives those levels for which the spins have been determined in other experiments. Many of those levels have a dominant  $2^+ \otimes f_{7/2}$  or  $3^- \otimes f_{7/2}$  structure, i.e., they are members of the one-phonon-particle multiplets. As noted above the strengths of these low-lying transitions have relatively large systematic errors due to the uncertainty of the photon-flux calibration at energies below 2 MeV.

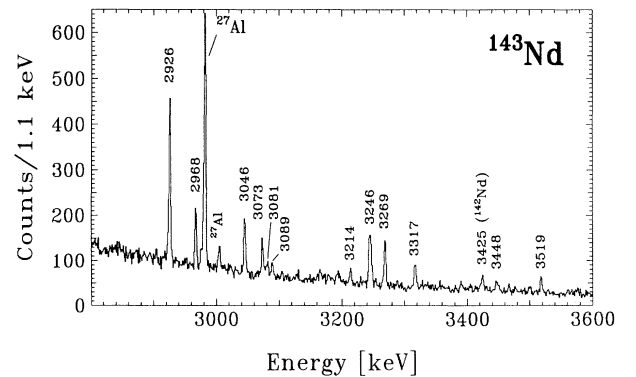


FIG. 4. NRF spectrum of  $^{143}\text{Nd}$  between 2.8 and 3.6 MeV. The strong line at 2.982 MeV belongs to the  $^{27}\text{Al}$  calibration standard.

(a) The  $9/2^-$  levels at 1407 and at 1739 keV. Both levels have been described as a mixed configuration consisting of the  $h_{9/2}$ -neutron excitation and the  $9/2^-$  member of the  $f_{7/2} \otimes 2^+$  multiplet [21]. (This multiplet arises from the coupling of the  $f_{7/2}$  neutron and the quadrupole vibration at 1576 keV in the core nucleus  $^{142}\text{Nd}$ .) The 1407-keV state has a ground-state decay width  $\Gamma_0=8.6\pm 2.8$  meV which corresponds to a half-life  $T_{1/2}=53_{-13}^{+26}$  fs. The excitation at 1739 keV has a ground-state decay width  $\Gamma_0=7.1\pm 2.0$  meV. Including a 2% branching to the 1431-keV level, as observed by Wrzesinski *et al.* [21], we obtain  $T_{1/2}=63_{-14}^{+25}$  fs.

(b) The  $11/2^-$  level at 1431 keV. This is the only quadrupole excitation observed in our  $(\gamma, \gamma')$  experiment. It results from the coupling of the  $f_{7/2}$  neutron to the  $2^+$  vibration in  $^{142}\text{Nd}$ . From the integrated cross section  $I_s=18.9\pm 6.4$  eV b we calculate a half-life  $T_{1/2}=68_{-17}^{+33}$  fs. This value should be compared to Coulomb-excitation experiments performed by Dragulescu *et al.* [27] yielding a half-life  $T_{1/2}=135\pm 14$  fs.

(c) The  $5/2^-$  levels at 1555 keV and at 1911 keV. The former level has been interpreted as the  $J = 5/2$  member of the  $f_{7/2} \otimes 2^+$  multiplet. Wrzesinski *et al.* observed an 11% branching to the  $3/2^-$  level at 742 keV. With this branching we deduce a half-life  $T_{1/2}=186_{-43}^{+70}$  fs which is in agreement with the findings of Wrzesinski *et al.* ( $T_{1/2} < 500$  fs). The 1911-keV level has a large  $f_{7/2} \otimes 4^+$  component. We determine a half-life  $T_{1/2}=67_{-14}^{+24}$  fs.

(d) The  $7/2^-$  level at 1851 keV. This is another member of the  $f_{7/2} \otimes 2^+$  multiplet; its half-life is  $T_{1/2}=50_{-11}^{+19}$  fs.

We note that we found another hitherto unknown level in this energy region at 1690 keV. As discussed above we are not able to determine the spin, but the decay width ( $g\Gamma_0=10.9\pm 3.6$  meV) is comparable to those observed for the states discussed above.

Discussing these  $2^+$ -particle excitations we note that the  $2^+$  level at 1576 keV in the core nucleus  $^{142}\text{Nd}$  has an integrated cross section  $I_s=29.6\pm 7.7$  eV b which yields a half-life  $T_{1/2}=117_{-24}^{+40}$  fs. This value was observed in an experiment by Pitz *et al.* [16] and is in agreement with the value deduced from the  $^{142}\text{Nd}$ -target contamination in the  $^{143}\text{Nd}$  target in the present experiment.

(e) The  $5/2^+$  levels at 1995 and at 2222 keV. Those levels have integrated cross sections of  $I_s=4.1\pm 1.7$  and  $3.6\pm 0.9$  eV b, respectively. The former state can be described by a dominant  $3^- \otimes f_{7/2}$  structure whereas the latter has a significant contribution from the  $\nu d_{5/2}^{-1}$ -hole excitation (see Ref. [21]). We note that both levels have very short half-lives  $T_{1/2} < 0.1$  ps.

(f) The  $9/2^+$  level at 2011 keV. This level is a member of the  $3^- \otimes f_{7/2}$  multiplet. The level is strongly excited in our experiment and decays to the ground state only. Its half-life is  $T_{1/2}=27_{-2}^{+3}$  fs which corresponds to  $B(E1)\uparrow=(2.75 \pm 0.25) \times 10^{-3} e^2 \text{fm}^2$ .

(g) The  $7/2^+$  level at 2091 keV. This is another member of the  $3^- \otimes f_{7/2}$  multiplet. We observed only the ground-state transition because the transition to the  $5/2^-$  state at 1555 keV and of the transition to the  $9/2^-$  state at 1407 keV (each of which is three times stronger than

the ground-state transition) are located at energies where the exponentially increasing bremsstrahlung background makes their detection virtually impossible. Including the branchings from Ref. [21] the ground-state decay width increases to  $\Gamma_0=15\pm 8$  meV. Therefore the lifetime of this state is comparable to the lifetime of the  $9/2^+$  level at 2011 keV, even though the errors are fairly large.

(h) The  $(7/2)^\pi$  level at 2317 keV and the  $(9/2)^+$  level at 2558 keV. The structure of these states is unknown. Both have been observed in the  $^{140}\text{Ce}(\alpha, n\gamma)^{143}\text{Nd}$  and in the  $^{143}\text{Nd}(p, p')^{143}\text{Nd}$  experiments [21,22]. The latter state has a very short half-life  $T_{1/2}=25_{-4}^{+5}$  fs.

## B. States with unknown spins

Besides the levels discussed above we excited a number of hitherto unknown levels. As we explained in the second section it was impossible to determine the spin of these states in our NRF experiments. Therefore they may have spins ranging from  $J = 3/2$  to  $J = 11/2$ . From our systematic studies on numerous even-even nuclei where the spins can be determined unambiguously and from the comparison of levels excited in our experiments on odd- $A$  nuclei with other experiments we know that nearly exclusively dipole excitations are populated. In the case of  $^{143}\text{Nd}$  this means that the observed levels are likely to be  $J = 5/2, 7/2, \text{ or } 9/2$ .

One can distinguish two groups of new levels in the experiment:

(a) Four levels between 2.4 and 2.8 MeV;

(b) 13 levels between 2.8 and 3.8 MeV for which we assume a two-phonon-particle  $2^+ \otimes 3^- \otimes f_{7/2}$  structure. Besides those two groups we observed one additional level at 1.690 MeV which was discussed above. We note that no level was observed above 3.8 MeV up to the endpoint energy of 4 MeV.

The structure of the first group of levels is not very clear. In  $(\gamma, \gamma')$  experiments on the neighboring even-even nucleus  $^{142}\text{Nd}$  two  $2^+$  levels at 2.385 and 2.846 MeV and one  $1^+$  level at 2.583 MeV had been observed [16]. In  $^{143}\text{Nd}$  the four states at 2.415, 2.493, 2.554, and 2.629 MeV have similar cross sections around 4 eV b.

With the coupling of the quadrupole with the octupole vibration in the core nucleus  $^{142}\text{Nd}$  one creates a multiplet of states with  $J^\pi=1^-$  to  $5^-$ . In the neighbor nucleus  $^{143}\text{Nd}$  the additional neutron can couple to these excitations and create 31 two-phonon-particle states. Fifteen of these states have the appropriate spin to be populated by dipole transitions from the ground state if one assumes strong mixing between states with equal spin. The excitation energy should be close to the energy of the multiplet in the core nucleus, i.e., around 3.4 MeV. The details of the core-particle coupling will be discussed in the next section. Here we will concentrate on possible candidates for these two-phonon-particle states observed in the experiment.

The strongest excitation observed in this experiment was in fact observed near 3.4 MeV, i.e., at 2.926 MeV with an integrated cross section of  $I_s=35.6\pm 2.5$  eV b. This amounts to a reduced transition strength from the

ground state of  $B(E1)\uparrow = (3.0 \pm 0.2) \times 10^{-3} e^2 \text{fm}^2$ . Another strong transition was observed from the level at 3.246 MeV with  $I_s = 66.1 \pm 6.0 \text{ eV b}$ . This results in a reduced transition strength from the ground state of  $B(E1)\uparrow = (1.84 \pm 0.17) \times 10^{-3} e^2 \text{fm}^2$ .

The level at 3.214 MeV shows a branching to the first excited state at 742 keV of  $\Gamma/\Gamma_0 = 4.0 \pm 0.9$  with  $\Gamma$  and  $\Gamma_0$  as defined in Eqs. (1) and (2). The strength distribution for these and the other states between 2.8 and 3.8 MeV is shown in the upper part of Fig. 6 below. As explained in Sec. II we give the spin and energy reduced ground-state decay widths times a factor  $b$  which converts the strengths into units of  $10^{-3} e^2 \text{fm}^2$ .

If one assumes that all observed transitions between 2.8 and 3.8 MeV have electric dipole character, one obtains

$$\begin{aligned} \sum B(E1)\uparrow &= \sum_{J_n} B(E1; J_0 \rightarrow J_n) \\ &= (13.6 \pm 1.8) \times 10^{-3} e^2 \text{fm}^2. \end{aligned} \quad (11)$$

Later we will see how this value can be compared to the  $E1$  strength measured in the core nucleus  $^{142}\text{Nd}$ .

#### IV. THEORETICAL CALCULATIONS

##### A. Level energies

In order to describe the experimental data, we performed theoretical calculations in a simple core coupling model with quadrupole-quadrupole ( $QQ$ ) interaction. An octupole-octupole ( $T_3T_3$ ) interaction was also included but only a few states of the phonon $\otimes$ particle multiplets were affected considerably. As a good description of the core nucleus  $^{142}\text{Nd}$  is needed, we compute the energies and quadrupole moments of  $^{142}\text{Nd}$  using the  $sdf$  interacting boson model [28]. The Hamiltonian for the core can be written as

$$\hat{H} = \epsilon_d \hat{n}_d + \epsilon_f \hat{n}_f - \kappa \hat{Q} \cdot \hat{Q}, \quad (12)$$

where  $\hat{n}_d$  and  $\hat{n}_f$  count the number of quadrupole and octupole phonons, respectively.  $\hat{Q}$  is the quadrupole operator and is written in terms of boson creation and annihilation operators as

$$\hat{Q}^{(2)} = (s^\dagger \tilde{d} + s d^\dagger)^{(2)} + \chi_{sd} (d^\dagger \tilde{d})^{(2)} + \chi_f (f^\dagger \tilde{f})^{(2)}. \quad (13)$$

We used the harmonic approximation for the energies of the one-phonon states and used the  $QQ$  interaction to compute the energy splitting of the  $2^+ \otimes 3^-$  multiplet. The coupling constant  $\kappa$  was determined from the experimentally known energy of the  $1^-$  member of the two-phonon multiplet and the presumed multiplet centroid energy  $E_{\text{centr}} = E_{2^+} + E_{3^-}$ . No other states besides the  $2^+$ ,  $3^-$ , and  $2^+ \otimes 3^-$  multiplet were included in the model space.

At the same time the coupling of the odd neutron to the one-phonon states in the core was computed via the coupling Hamiltonian

$$\hat{H}_C = \tilde{\kappa} \hat{Q} \hat{q}_{s.p.} + \tilde{\kappa}' \hat{T}_3 \hat{t}_{3s.p.} + \eta (a^\dagger a) (\hat{n}_d + \hat{n}_f). \quad (14)$$

In order to fix all parameters a simultaneous fit of  $^{142}\text{Nd}$  and  $^{143}\text{Nd}$  was performed.

We included the  $f_{7/2}$ ,  $p_{3/2}$ ,  $h_{9/2}$ , and  $i_{13/2}$  single-particle states in the calculations. The single-particle energies were fixed from the observed splittings of states having large amplitudes of the single-particle states, e.g., the two lowest  $9/2^-$  levels for the  $h_{9/2}$  amplitudes. They are in good agreement with those obtained in a detailed study of the  $N = 83$  isotones [29].

The computed one-phonon particle multiplets served to fix the core-particle  $QQ$  interaction strength  $\tilde{\kappa}$  and the quadrupole moments of the core phonon states. In Fig. 5 we show the experimental one-phonon-particle multiplets together with the computed states. A satisfactory overall agreement was achieved. We adjusted  $\eta$  so that the one-phonon-particle multiplets were shifted down by 0.2 MeV. This shift does not alter the structure of the multiplets, but it greatly improves the correspondence between experimental and theoretical states. The actual calculations were performed using the computer code COUPLIN by Dönaau [30] and were carefully checked against similar calculations using the computer code PCQ\_ODD by Heyde and Brussaard [31].

##### B. Transition strengths

Electric dipole transitions from the ground state to the two-phonon multiplet were also computed. We exploited

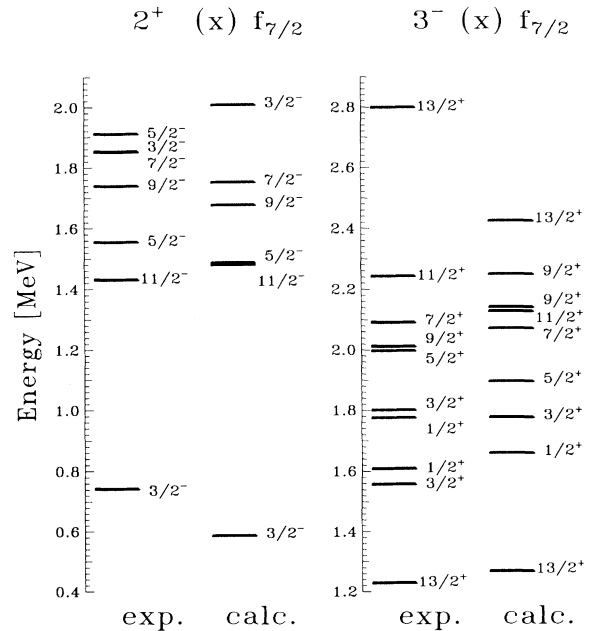


FIG. 5. Computed and experimental low-lying one-phonon-particle multiplets. The overall agreement is good. As we did not include the  $g_{9/2}$  single-particle level, the computed energies of the  $9/2^+$  levels are too high.

the fact that  $^{143}\text{Nd}$  has one neutron outside a magic core. The odd neutron should therefore be coupled weakly to the core and we can assume that the only contribution to the  $B(E1)$  values from the state  $J$  to the ground state  $7/2^-$  comes from the underlying  $1^- \rightarrow 0^+$  transition in the core. An additional contribution to the  $E1$  transitions comes from the  $3_1^- \rightarrow 2_1^+$  transition of the core which is of similar magnitude to the  $1^- \rightarrow 0^+$  transition. However, in the states near 3 MeV in  $^{143}\text{Nd}$  the  $3_1^- \rightarrow 2_1^+$  contribution to the total  $B(E1)$  value is only of the order of a few percent or less.  $E1$  transitions between different single-particle states were neglected.

As we want to compare the theoretical values with these from the experiment we give  $B(E1)\uparrow$  values. Following the arguments presented in Sec. II, these can be derived from the  $(\gamma, \gamma')$  experiment without needing to know the spins of the excited states. Figure 6 shows the distribution of  $E1$  strength up to 4 MeV. One can clearly see a good reproduction of the computed and the experimental  $E1$  strength distributions. The calculated  $E1$  strength is concentrated between 2.8 and 3.8 MeV. The summed transition strength as well as the fragmentation reproduce the experimental situation rather well. In the calculations no strong  $E1$  transitions were found above 4 MeV.

In our previous Letter [24] the  $E1$  distribution was computed under the assumption that only the  $1^- \rightarrow 0^+$   $E1$  transition of the core led to large  $E1$  transitions of the coupled system. We also neglected the influence of single-particle states other than  $f_{7/2}$ . As was expected, the inclusion of more single-particle levels and the correct treatment of the  $3^- \rightarrow 2^+$  contribution to the  $E1$  values significantly improved the correspondence between the experimental and the computed  $E1$  strength distribution.

If the  $B(E1)$  values of all states containing a  $1^- \otimes f_{7/2}$  amplitude are summed up, one finds

$$\begin{aligned} \sum_{J_n} B(E1)\uparrow &= \sum_{J_n} B(E1; J_0 \rightarrow J_n)_{^{143}\text{Nd}} \\ &= B(E1; 0^+ \rightarrow 1^-)_{^{142}\text{Nd}}, \end{aligned} \quad (15)$$

where  $J_0 = 7/2^-$ . This sum rule valid for extremely weak particle-core coupling is easily derived and well known. For the experimental two-phonon-particle states in  $^{143}\text{Nd}$  one finds the experimental value

$$\sum_{J_n} B(E1)\uparrow_{^{143}\text{Nd}} = (13.6 \pm 1.8) \times 10^{-3} e^2 \text{fm}^2 \quad (16)$$

[cf. Eq. (11)]. According to Eq. (15) this value should be compared to the value in the core  $^{142}\text{Nd}$ :

$$B(E1; 0^+ \rightarrow 1^-)_{^{142}\text{Nd}} = (16.3 \pm 2.4) \times 10^{-3} e^2 \text{fm}^2. \quad (17)$$

If one takes into account that the ground-state wave function of  $^{143}\text{Nd}$  contains only a 75%  $0^+ \otimes f_{7/2}$  component [33], we expect a  $\sum B(E1)\uparrow$  value of

$$\sum_{J_n} B(E1)\uparrow_{^{143}\text{Nd}} = (12.2 \pm 1.8) \times 10^{-3} e^2 \text{fm}^2. \quad (18)$$

As these values are among the largest  $B(E1)$  values known, we find a good agreement between theory and experiment, again strongly supporting the argument in favor of the proposed underlying two-phonon-particle structure of the observed levels around 3 MeV. It is worth noting that the calculations show no significant amount of  $M1$  strength in the energy region between 2.8 and 4 MeV. This also supports our assumption of positive parities for the observed levels.

## V. CONCLUSION

A nuclear resonance fluorescence experiment was performed on the odd- $A$  nucleus  $^{143}\text{Nd}$ . Absolute transition widths, cross sections, and lifetimes were extracted for a number of states below 4 MeV. The levels between 2.8 MeV and 4 MeV have large  $B(E1)\uparrow$  values. These states are interpreted as members of a  $2^+ \otimes 3^- \otimes f_{7/2}$  multiplet which was observed in  $^{143}\text{Nd}$  for the first time. The  $\sum B(E1)\uparrow$  value exhausts the sum rule for weak particle-core coupling and supports this interpretation. Calculations in a core-coupling model were performed and were able to reproduce the main features of the observed levels and the observed distribution of  $B(E1)$  strength among them.

## ACKNOWLEDGMENTS

We wish to thank S. Albers, F. Dönau, A. Faessler, A. Gelberg, R. V. Jolos, B. R. Mottelson, N. Pietralla, A. Richter, and L. Trache for many stimulating and

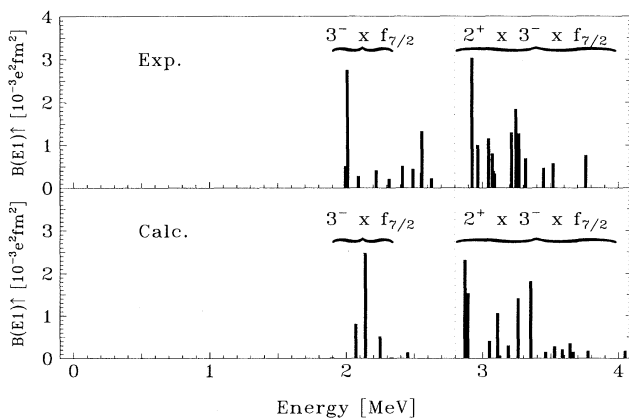


FIG. 6. Experimental strength distribution in  $^{143}\text{Nd}$  between 0 and 4 MeV. If the transitions have  $E1$  character one finds  $b\Gamma_0^{\text{red}} = B(E1; J_0 \rightarrow J_n)$ , where  $\Gamma_0^{\text{red}} = \Gamma(J_0 \rightarrow J_n) E_r^{-3}$  and  $b = 0.9553 \times 10^{-3} e^2 \text{fm}^2 \text{MeV}^3 / \text{meV}$ . In the experimental analysis pure dipole character was assumed for all transitions.

enlightening discussions. Two of us (R.-D.H. and A.Z.) wish to thank the Institut für Strahlenphysik in Stuttgart for the kind hospitality during numerous stays in Stuttgart. One of us (A.M.O.) gratefully acknowledges

the support of the Deutscher Akademischer Austauschdienst for her stay in Cologne. This work was supported in part by the Deutsche Forschungsgemeinschaft under Contracts No. Br 799-33/34 and No. Kn 154-21.

- 
- [1] P. D. Cottle, *Phys. Rev. C* **42**, 1264 (1990).
- [2] T. Guhr, K.-D. Hummel, G. Kilgus, D. Bohle, A. Richter, C. W. de Jager, H. de Vries, and P. K. A. de Witt Huberts, *Nucl. Phys.* **A501**, 95 (1989).
- [3] F. Iachello, *Phys. Lett.* **160B**, 1 (1985).
- [4] W. Urban, R. M. Lieder, W. Gast, G. Hebbinghaus, A. Krämer-Flecken, T. Morek, T. Rzaca-Urban, W. Nazarewicz, and S. L. Tabor, *Phys. Lett. B* **200**, 424 (1988).
- [5] P. A. Butler and W. Nazarewicz, *Nucl. Phys.* **A533**, 249 (1991).
- [6] P. D. Cottle and D. A. Bromley, *Phys. Lett. B* **182**, 129 (1986).
- [7] W. Donner and W. Greiner, *Z. Phys.* **197**, 440 (1966).
- [8] A. Zilges, P. von Brentano, H. Friedrichs, R. D. Heil, U. Kneissl, S. Lindenstruth, H. H. Pitz, and C. Wesselborg, *Z. Phys. A* **340**, 155 (1991).
- [9] A. Zilges, P. von Brentano, and A. Richter, *Z. Phys. A* **341**, 489 (1992).
- [10] P. von Brentano, A. Zilges, R. D. Heil, R.-D. Herzberg, U. Kneissl, H. H. Pitz, and C. Wesselborg, *Nucl. Phys.* **A557**, 593c (1993).
- [11] P. O. Lipas, *Nucl. Phys.* **82**, 91 (1966).
- [12] A. Raduta, A. Sandulescu, and P. O. Lipas, *Nucl. Phys.* **A149**, 11 (1970).
- [13] P. Vogel and L. Kocbach, *Nucl. Phys.* **A176**, 33 (1971).
- [14] F. R. Metzger and V. K. Rasmussen, *Bull. Am. Phys. Soc.* **18**, 1386 (1972).
- [15] F. R. Metzger, *Phys. Rev. C* **14**, 543 (1976); **18**, 1603 (1978); **18**, 2138 (1978).
- [16] H. H. Pitz, R. D. Heil, U. Kneissl, S. Lindenstruth, U. Seemann, R. Stock, C. Wesselborg, A. Zilges, P. von Brentano, S. D. Hoblit, and A. M. Nathan, *Nucl. Phys.* **A509**, 587 (1990).
- [17] R. A. Gatenby, J. R. Vanhoy, E. M. Baum, E. L. Johnson, S. W. Yates, T. Belgya, B. Fazekas, A. Veres, and G. Molnár, *Phys. Rev. C* **41**, R414 (1990).
- [18] E. Müller-Zanotti, R. Hertenberger, H. Kader, D. Hofer, G. Graw, Gh. Cata Danil, G. Lazzari, and P. F. Bortignon, *Phys. Rev. C* **47**, 2524 (1993).
- [19] R. A. Gatenby, E. L. Johnson, E. M. Baum, S. W. Yates, D. Wang, J. R. Vanhoy, M. T. McEllistrem, T. Belgya, B. Fazekas, and G. Molnár, *Nucl. Phys.* **A560**, 633 (1993).
- [20] S. Albers (private communication).
- [21] J. Wrzesinski, A. Clauberg, C. Wesselborg, R. Reinhardt, A. Dewald, K. O. Zell, P. von Brentano, and R. Broda, *Nucl. Phys.* **A515**, 297 (1990).
- [22] L. Trache, J. Wrzesinski, C. Wesselborg, A. Clauberg, K. O. Zell, R. Reinhardt, P. von Brentano, D. Bazzacco, G. P. A. Berg, W. Hürlimann, J. Meissburger, and J. L. Tain, *Nucl. Phys.* **A492**, 23 (1989).
- [23] P. Kleinheinz, J. Styczen, M. Piiparinen, J. Blomqvist, and M. Kortelahti, *Phys. Rev. Lett.* **48**, 1457 (1982).
- [24] A. Zilges, R.-D. Herzberg, P. von Brentano, F. Dönau, R. D. Heil, R. V. Jolos, U. Kneissl, J. Margraf, H. H. Pitz, and C. Wesselborg, *Phys. Rev. Lett.* **70**, 2880 (1993).
- [25] H. H. Pitz, U. E. P. Berg, R. D. Heil, U. Kneissl, R. Stock, C. Wesselborg, and P. von Brentano, *Nucl. Phys.* **A492**, 411 (1989).
- [26] N. Pietralla, P. von Brentano, R.-D. Herzberg, A. Zilges, I. Bauske, O. Beck, U. Kneissl, J. Margraf, H. Maser, and H. H. Pitz, *Phys. Rev. C* **51**, 1021 (1995).
- [27] E. Dragulescu, M. Ivascu, R. Mihiu, D. Popescu, G. Semencescu, V. Paar, and D. Vretenar, *Nucl. Phys.* **A419**, 148 (1984).
- [28] F. Iachello and A. A. Arima, *The Interacting Boson Model* (Cambridge University Press, Cambridge, England, 1987).
- [29] A. M. Oros, L. Trache, P. von Brentano, K. Heyde, and G. Graw, *Phys. Scr.* (in press).
- [30] F. Dönau, *Z. Phys. A* **293**, 31 (1979); F. Dönau and S. Frauendorf, *Phys. Lett.* **71B**, 263 (1977).
- [31] K. Heyde and P. J. Brussaard, *Nucl. Phys.* **A104**, 81 (1967).
- [32] L. K. Peker, *Nucl. Data Sheets* **64**, 429 (1991).
- [33] J. C. Veefkind, D. Spaargaren, J. Blok, and K. Heyde, *Z. Phys. A* **275**, 55 (1975).